JOURNAL OF GEOPHYSICAL RESEARCH, VOL. 112, D23S17, doi:10.1029/2006JD008037, 2007



# Direct shortwave radiative forcing of sulfate aerosol over Europe from 1900 to 2000

E. Marmer,[1,2] B. Langmann,[1,3] H. Fagerli,[4] and V. Vestreng[4]

Received 15 September 2006; revised 23 May 2007; accepted 28 June 2007; published 2 October 2007.

[1] On the basis of historical simulations of the atmospheric distribution of sulfate aerosol over Europe, we have estimated the evolution of the direct shortwave radiative forcing due to sulfate aerosol from 1900 to the present day. Following the trend of atmospheric sulfate burden, the radiative forcing reaches its peak in the 1980s. Since then, environmental policies regulating $SO_x$ emissions successfully reduced the atmospheric load. On average, the forcing of the year 2000, representing present day, equals that of the 1950s. Spatially, the forcing maxima experienced a shift from the northwest to the southeast during the century. The ship emissions of sulfur keep increasing since the 1980s, hence their relative contribution to the sulfate load and radiative forcing constantly increased, from 3% in the 1980s to over 10% in the year 2000. Forcing is strongest during summertime, with a seasonal mean of $-2.7$ W m$^{-2}$ in the 1980s and $-1.2$ W m$^{-2}$ in summer 2000. The mean forcing efficiency is slightly reduced from $-246$ W (g sulfate)$^{-1}$ in the 1900s to $-230$ W (g sulfate)$^{-1}$ in the year 2000, and it declines with changed geographical distribution of sulfur emissions.

**Citation:** Marmer, E., B. Langmann, H. Fagerli, and V. Vestreng (2007), Direct shortwave radiative forcing of sulfate aerosol over Europe from 1900 to 2000, *J. Geophys. Res.*, *112*, D23S17, doi:10.1029/2006JD008037.

## 1. Introduction

[2] Anthropogenic emissions have caused serious environmental problems in Europe since the beginning of industrialization, contributing to soil, water and air pollution. Air pollution affects climate through absorbing and scattering aerosol particles, which can warm or cool the Earth-atmosphere system. Emissions of $SO_x$ and black carbon are particularly relevant for the climate.

[3] $SO_x$, emitted mostly as $SO_2$ gas, is converted in the atmosphere via gaseous and aqueous chemical reaction to sulfate aerosol. Sulfate aerosol has an impact on climate via direct and indirect radiative forcing. For sulfate aerosol, the direct effect results from scattering of incoming solar radiation back to space. The indirect effect results from the ability of the sulfate aerosol particles to act as cloud condensation nuclei, resulting in more but smaller cloud droplets, increasing the cloud albedo [*Twomey*, 1974]. On the other hand, smaller cloud droplets can suppress precipitation, prolonging the life time of the cloud and the aerosol [*Albrecht*, 1989]. The combination of these effects and their feedbacks is up to now poorly understood [*Intergovernmental Panel on Climate Change* (*IPCC*), 2001a].

[4] Additional uncertainties exist about the direct, semi-direct and indirect effects of black carbon. Black carbon strongly absorbs the solar radiation and warms the aerosol layer. It can trap more energy than is lost by scattering to space to overall warm the Earth-atmosphere system. Absorption of solar radiation by black carbon particles in clouds can evaporate cloud droplets reducing cloud cover [*Ackerman et al.*, 2000]. Further, black carbon particles in cloud droplets can reduce the cloud albedo [*Krüger and Grassl*, 2002] and can act as ice nuclei [*DeMott et al.*, 1999].

[5] Considering the climate impact of both sulfate and black carbon aerosols presents yet another problem: for newly released particles their climate impact can be treated individually, whereas aged particles are internally mixed. Internally mixed particles have different optical and hygroscopic properties depending on their age and chemical composition [*Lesins et al.*, 2002]. *Haywood et al.* [1997], *Myhre et al.* [1998] and *Lesins et al.* [2002] showed that an internal mixture of sulfate and black carbon results in substantially different forcing than an external mixture.

[6] In this study we investigate the historical evolution of the aerosol radiative forcing over Europe during the 20th century. We look at the direct forcing only, because it is the best understood aerosol effect. The study is further limited to sulfate aerosol, since a consistent historical emission inventory of black carbon in Europe in suitable resolution is not yet available.

[7] *Myhre et al.* [2001] estimated the averaged global radiative forcing evolution from 1750 to 1995, utilizing a radiation transfer model. All known radiative forcings, greenhouse gases, ozone, anthropogenic and natural aerosols (including sulfate and black carbon), and solar irradi-

[1]Max Planck Institute for Meteorology, Hamburg, Germany.
[2]Now at Joint Research Centre, Ispra, Italy.
[3]Now at Department of Experimental Physics, National University of Ireland, Galway, Ireland.
[4]Norwegian Meteorological Institute, Oslo, Norway.


0148-0227/07/2006JD008037$09.00

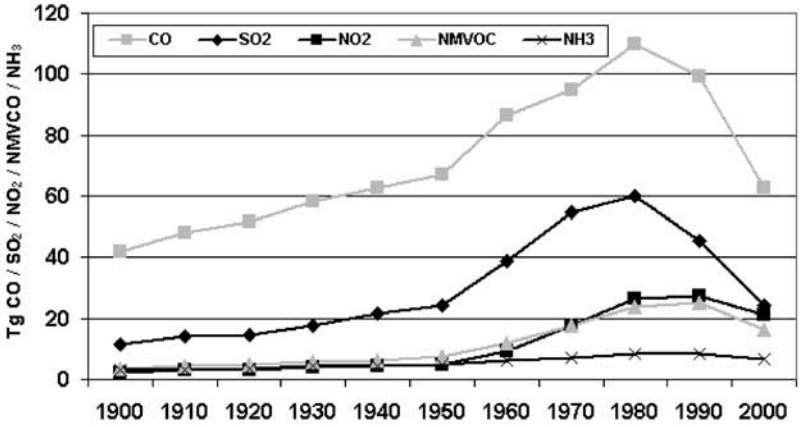


**Figure 1.** European emissions included in the EMEP domain (CO, $SO_2$, $NO_2$, NMVOC, $NH_3$, natural and anthropogenic (Tg/Year)).

ance radiation, were considered. The global mean direct aerosol forcing was computed assuming internal and external aerosol mixtures. The evolution of the sulfate aerosol forcing was calculated scaling to global mean $SO_2$ emissions. This study points out the increasing importance of the anthropogenic aerosol forcing for the past 100 years. The global mean direct radiative forcing of sulfate of $-0.05$ W $m^{-2}$ is given for the 1900s, its value doubled in 1945, almost constantly increasing to $-0.36$ W $m^{-2}$ by 1995, with only a minor decrease during the 1980s.

[8] *Boucher and Pham* [2002] computed the direct and indirect sulfate aerosol forcing over the period 1850 to 1990 applying a global GCM. They focused on sulfate aerosol only, because more information was available for sulfur sources than for other aerosol species. They found that the global direct sulfate forcing has increased from near zero [1850] to $-0.42$ W $m^{-2}$ in 1990, with nearly constant forcing efficiency of $-150$ W(g sulfate)$^{-1}$ (ratio of the radiative forcing to the anthropogenic sulfate burden). The global forcing was found to be fairly constant between 1980 and 1990 because of emissions reduction in the US and Europe, with a spacial shift from the US, Europe, Russia and the North Atlantic to Southeast Asia and the Indian and Pacific Oceans.

[9] Another study on the trend in tropospheric aerosol loads and the direct radiative forcing was carried out by *Tegen et al.* [2000]. The global trend of the atmospheric load and forcing of sulfate and carbonaceous aerosols from fossil fuel burning as well as soil, dust and sea salt from 1950 to 1990 was constructed. In 1950, the global averaged optical thickness of anthropogenic sulfate aerosol (0.005) was found to be smaller than that of natural sulfate (0.007), it more than doubled by 1990s (0.011). Globally, a range of top-of-atmosphere direct forcing of $-0.5$ to $+0.1$ W $m^{-2}$ was found because of the uncertainty in the contribution of the black carbon aerosol.

[10] For our study we have utilized a regional model, which provides a better resolution than the earlier performed global simulations, allowing us to have a closer look at different regions in Europe. In order to better demonstrate the regional differences, we have calculated sulfate direct forcing for five selected areas in Europe, representing different geographical and atmospherical conditions, and discuss the different trends for each of these areas. Ship emissions is the only constantly growing source of sulfur in Europe. A sensitivity study without ship emissions investigates the trend of their relative contribution to the direct radiative forcing during the past century. The results of the present study serve as a baseline for future investigations on aerosol climate impact evolution over Europe, which should include black carbon.

## 2. Emissions

[11] In this section, we describe the emission data used in the assessments with the EMEP Unified model [*Simpson et al.*, 2003a] discussed in the next chapter. The emission data has been collected from different sources depending on the availability of emission years, compounds, sectoral breakdown, resolution and quality considerations. The emissions are depicted on the basis of emission levels and sector distribution, spatial and temporal distribution and information about natural and shipping emissions (Figure 1 and Table 1).

### 2.1. Emission Levels

[12] The anthropogenic emission input data of $SO_2$, $NO_x$, $NH_3$, CO and NMVOC from 1980 to 2003 are based as far as possible upon emissions reported per sector and grid officially reported to the Convention on Long-Range Transboundary Air Pollution [*Vestreng et al.*, 2004].

[13] For the period prior to 1980, we have used three different sources of information (Table 2) in consistency with EMEP data for the years 1980–2000.

[14] An evaluation of the *van Aardenne et al.* [2001] inventory for $SO_2$ reveals that this inventory has rather a constant level of emissions between 1980 and 1990, while *Lefohn et al.* [1999] show an increase of European sulfur emissions in the 1980s. We have compared the *van Aardenne et al.* [2001] and *Mylona* [1996] emission inventories (excluding the former USSR/CIS emission estimates), and find that there are substantial differences in emission levels and trends particularly from 1950 onward. *Mylona* [1996] emissions per country show close agreement with the EMEP official emissions which have been validated by models and measurements between 1980–2000 (section 3.2), hence *Mylona* [1996] was our preferred choice for $SO_2$ inventory.

**Table 1.** European Emissions Included in the EMEP Domain, Natural and Anthropogenic[a]

| | $SO_x$ ($TgSO_2$) | | | $NO_x$ ($TgNO_2$) | | | NMVOC | | | $NH_3$ | | | CO | | |
|---|---|---|---|---|---|---|---|---|---|---|---|---|---|---|---|
| Year | Land | Ships | Other[b] | Land | Ships | Other[b] | Land | Ships | Other[b] | Land | Ships | Other[b] | Land | Ships | Other[b] |
| 2000 | 17.36 | 2.72 | 4.16 | 16.95 | 3.85 | 0.32 | 16.01 | 0.081 | 0.39 | 6.06 | - | 0.56 | 61.08 | 0.33 | 1.25 |
| 1990 | 39.19 | 2.13 | 4.16 | 23.84 | 3.01 | 0.32 | 24.55 | 0.081 | 0.39 | 7.92 | - | 0.56 | 97.55 | 0.33 | 1.25 |
| 1980 | 54.16 | 1.66 | 4.16 | 23.81 | 2.35 | 0.32 | 23.47 | 0.050 | 0.40 | 8.04 | - | 0.56 | 108.13 | 0.20 | 1.31 |
| 1970 | 50.29 | 1.02 | 3.59 | 15.85 | 1.44 | 0.23 | 17.24 | 0.030 | 0.40 | 6.79 | - | 0.43 | 93.43 | 0.12 | 1.11 |
| 1960 | 34.93 | 0.57 | 3.23 | 8.07 | 0.81 | 0.18 | 11.99 | 0.017 | 0.14 | 5.74 | - | 0.33 | 85.98 | 0.07 | 0.94 |
| 1950 | 21.10 | 0.32 | 3.03 | 4.37 | 0.45 | 0.15 | 7.26 | 0.009 | 0.09 | 4.77 | - | 0.29 | 66.12 | 0.04 | 0.75 |
| 1940 | 18.38 | 0.36 | 2.97 | 4.10 | 0.33 | 0.13 | 6.18 | 0.007 | 0.07 | 4.09 | - | 0.18 | 62.00 | 0.03 | 0.64 |
| 1930 | 14.37 | 0.29 | 2.90 | 3.35 | 0.41 | 0.13 | 5.47 | 0.009 | 0.06 | 4.05 | - | 0.16 | 57.77 | 0.04 | 0.52 |
| 1920 | 11.59 | 0.18 | 2.88 | 2.86 | 0.26 | 0.12 | 4.61 | 0.005 | 0.05 | 3.30 | - | 0.12 | 50.99 | 0.02 | 0.44 |
| 1910 | 10.92 | 0.19 | 2.87 | 2.60 | 0.27 | 0.11 | 4.17 | 0.006 | 0.05 | 2.78 | - | 0.10 | 47.79 | 0.02 | 0.38 |
| 1900 | 8.45 | 0.12 | 2.86 | 2.09 | 0.17 | 0.11 | 3.46 | 0.00 | 0.04 | 3.10 | - | 0.09 | 41.52 | 0.02 | 0.33 |

[a]Unit is Tg/Year.
[b]Other, emissions from North African and Asian areas within the EMEP domain. In addition natural emissions (volcanoes, approximately 2 Tg/Yr $SO_2$, and DMS, 0.8 Tg/Yr $SO_2$) are included for $SO_x$.

*Berglen et al.* [2007] concluded that model assessments performed with the EMEP inventory better reproduced the trends in observations 1985–2000 than the *Smith et al.* [2004] inventory. Emissions available in the EMEP database (http://webdab.emep.int/, and V. Vestreng and A. Semb, Nitrogen oxides emission inventories over Europe since the preindustial era, unpublished manuscript, 2006, hereinafter referred to as Vestreng and Semb, unpublished manuscript, 2006) show that the land based European sector emissions have been continuously reduced between 1980 and 1990, in accordance with *Mylona* [1996]. Thus we have relied on the European $SO_2$ inventory developed by *Mylona* [1996] despite that this inventory originally lacks the sectoral breakdown.

[15] The $SO_2$ inventory from *Mylona* [1996] were distributed according to EMEP 1980 sector distribution for SNAP (Selected Nomenclature for Air Pollutants, http://reports.eea.eu.int/EMEPCORINAIR3/en/) for the sectors 1, "Combustion in energy and transformation industries"; 2, "Nonindustrial combustion plants"; 3, "Combustion in manufacturing industries;" and 4, "Production processes," while sector 7, "Road transport," and 8, "Other mobile sources and machinery," are scaled according to the petroleum consumption.

[16] The $NO_x$ inventory included is developed by Vestreng and Semb (unpublished manuscript, 2006) by country and SNAP sector. This regionally developed $NO_x$ inventory compares much better with Alpine ice core data than the emissions from *van Aardenne et al.* [2001]. In particular the trend from 1950 to 1980 is much steeper in the Vestreng and Semb (unpublished manuscript, 2006) inventory as a result of the variable emission factors for road transport included.

[17] For $NH_3$, NMVOC and CO, we have included the *van Aardenne et al.* [2001]. In the case of CO and NMVOC there were to our knowledge no other inventories published. A historical emission inventory of ammonia including 12% natural emissions per European country for the years 1870, 1920, 1950 and 1980 has been provided by *Asman and Drukker* [1987]. Their anthropogenic emission inventory is comparable to that of *van Aardenne et al.* [2001] between 1950 and 1980 but estimates by *Asman and Drukker* [1987] exceed those of *van Aardenne et al.* [2001] before 1950, e.g., they estimate 20% more emissions in 1920 in Europe. Our choice of the *van Aardenne et al.* [2001] emission inventory for NH3 is due both to their more extensive database (more years included), and because their 1980 data compares better with officially reported data for Europe [*Vestreng et al.*, 2004].

[18] The *van Aardenne et al.* [2001] data is available in a $1^\circ \times 1^\circ$ degree grid and have been adapted onto SNAP source categories according to the EMEP 1980 sector split.

[19] The ships emissions of $SO_2$, $NO_x$, NMVOC and CO in the period from 1880 to 1975 have been assumed to be directly proportional to the registered tons associated with the steam and motor ships as detailed in *Mitchell* [1981]. For the years 1990 and 2000 emission estimates from *Lloyd's Register of Shipping* [1995, 1998, 1999] and from ENTEC [*Whall et al.*, 2002], respectively, are available. We have used the year 2000 emissions to downscale the ships emissions back to 1980, assuming a growth rate of 2.5% per year, or a factor 1.28 per decade [*Endresen et al.*, 2003].

[20] In addition, natural emissions of $SO_2$ from volcanoes and ocean phytoplankton (DMS) are included. The emissions from volcanoes are constant (2 Tg) throughout the period 1900–2000, equal to the Italian reported natural emissions of sulfur released from Mount Etna [*Vestreng et al.*, 2004]. The DMS inventory is constant over the years [*Tarrasón et al.*, 1995].

[21] Emissions from areas included in the EMEP domain but outside Europe (i.e., North African and some Asian countries), are from *van Aardenne et al.* [2001].

**Table 2.** Emission Data Characteristics for Inventories Included in This Study

| Emission Data Source | Pollutant | Years | Sectors | Resolution |
|---|---|---|---|---|
| *Mylona* [1996] | $SO_2$ | 1880–1990 | - | country/Europe/5 years interval |
| VestrengSemb (unpublished manuscript, 2006) | $NO_x$ | 1880–1985 | SNAP | country/Europe/5 years interval |
| *van Aardenne et al.* [2001] | $NH_3$, VOC, CO | 1880–1990 | EDGAR | $1^\circ \times 1^\circ$ global/10 years interval |
| *Vestreng et al.*, 2004 | $SO_2$, $NO_x$, $NH_3$, NMVOC, CO | 1980–2003 | SNAP | $50 \times 50$ $km^2$/Europe/annually |

### 2.2. Emission Distribution

[22] The temporal distribution of emissions has been done according to the Generation and Evaluation of Emission Data project (GENEMIS [*Friedrich and Reis*, 2004]), a subproject of EUROTRAC-2. (EUROTRAC-2 is the EUREKA Project on the Transport and Chemical Transformation of Environmentally Relevant Trace Constituents in the Troposphere over Europe; Second Phase (http://www.gsf.de/eurotrac/).) Monthly and daily factors are applied for the temporal emission distribution. The factors are specific to each pollutant, emission sector and county, taking into account the different climates and hence energy use across Europe.

[23] The heights of the stacks have changed significantly during the last century, which we have taken into account by defining a "tall stack" (1955–present) and a "low stack" (previous to 1955) period. During 1880–1945, stack heights were typical about 40 meters to "clear the roof tops and neighboring house" [*Brimblecombe*, 1987]. The stack heights increased to around 150 m in 1950–1975 as a result of increasing environmental concern ("tall stack policy"). In the model calculations, the effective emission heights of power plants and industry are moved one model layer closer to the ground in the low-stack period in an attempt to reproduce the historical distribution of stack heights. In both cases, the emissions rapidly become well mixed in the boundary layer and the effect is only minor.

[24] The emissions were distributed horizontally the following way. The *van Aardenne et al.* [2001] inventories were available per country with the present country borders. Scaling factors per country and sector were deduced by

$$\mathrm{f}_{Year}(\mathrm{country},\mathrm{sector}) = \mathrm{emission}_{Year}(\mathrm{country},\mathrm{sector}) / \mathrm{emission}_{1980}(\mathrm{country},\mathrm{sector})$$

and used to scale the EMEP 1980 emissions backward in time, but ensuring that the total emission fractions were kept. In this way, the finer resolution ($50 \times 50$ km$^2$) of the EMEP data could be kept and the evolution of the historic emissions included. In the data from *van Aardenne et al.* [2001], spatial distribution over the years is only different when the relative amount within the sectors change. Thus we loose no information when applying only the scaling factors as the sector information is kept.

[25] For $SO_2$ and $NO_x$, emission scaling factors were defined in the same way as for $NH_3$, VOC and CO. The historical emissions for $SO_2$ and $NO_x$ were available from 1880–1985 per country with country borders as they were historically. For instance, emissions are not available separately for the countries within the Former Soviet Union, and emissions from Austria did include emissions from the whole Austrian Empire before 1920. Thus we have made the following assumptions: The countries in the Former Soviet Union are scaled with the same factors from 1920 to 1980. East and West Germany are scaled separately back to 1950, but prior to this as a sum. The areas corresponding to Czech Republic and Slovakia are scaled with emissions for Former Czechoslovakia back to 1920. In the same period, Slovenia, Croatia, Bosnia and Herzegovina, Serbia and Montenegro and The Former Yugoslav Republic of Macedonia are scaled using the historic emissions of Former Yugoslavia. For the years prior to 1920, the changes of borders have been extensive and more crude assumption had to be made. Thus the uncertainties related to spatial distribution in this period are larger. Austria was a part of the Austrian Empire, including Czech Republic and Slovenia. For, e.g., 1910, Austria is scaled with

$$\frac{Austrianemissions(1920)}{Austrianemissions(1980)} \times \frac{AustrianEmpireemissions(1910)}{AustrianEmpireemissions(1920)},$$

where the Austrian Empire emissions for 1920 are estimated as the sum of emissions from Austria plus X $\times$ Former Czechoslovakia and Y $\times$ Former Yugoslavia. X has been defined as Czech Republic/(Czech Republic+Slovakia) for 1980, Y as Slovenia/(Slovenia, Croatia, Bosnia and Herzegovina, Serbia and Montenegro and The Former Yugoslav Republic of Macedonia) for 1980. X and Y have been defined separately for $SO_2$ and $NO_x$ emissions. The same procedure has been followed to define scaling factors for Hungary prior to 1920, as The Hungarian Kingdom included Hungary, Slovakia and Bosnia and Herzegovina. Before 1920, Russia included Poland, and United Kingdom included Ireland. Similar procedures were followed for these countries.

## 3. Model Setup

### 3.1. Unified EMEP Model

[26] The Eulerian EMEP model [*Simpson et al.*, 2003a] was utilized to determine the historical sulfate aerosol distribution. It is a multilayer atmospheric dispersion model designed for simulating the long-range transport of air pollution over several years. The model domain is centered over Europe and also includes most of the North Atlantic and the polar region. The model has 20 vertical layers in $\sigma$-coordinates below 100hPa. It is primarily intended for use with a horizontal resolution of $\sim 50 \times 50$ km$^2$ (at 60°N) in the EMEP polar stereographic grid. The chemical scheme uses about 140 reactions between 70 species. $SO_2$ is oxidized to sulfate both in gas phase with OH and in aqueous phase through $H_2O_2$, $O_3$ and $O_2$ catalyzed by metal ions, assuming a fixed pH value of 4.5. The sulfur chemistry is coupled to the photochemistry, thus changes in the oxidation capacity may change the $SO_2$ oxidation rate and vice versa. The partitioning between ammonia, ammonium, sulfate, nitrate and nitric acid is calculated using the EQSAM module detailed by *Metzger et al.* [2002a, 2002b].

[27] The dry deposition module makes use of a stomatal conductance algorithm which was originally developed for calculation of ozone fluxes, but which is now applied to all pollutants where stomatal control is important [e.g., *Simpson et al.*, 2003b; *Tuovinen et al.*, 2004]. Dry deposition of aerosol particles depends on their size, with the model version used here distinguishing between fine and coarse aerosols. Details of the formulation are given by *Simpson et al.* [2003a]. Parameterization of the wet deposition processes in the EMEP model includes both in-cloud and subcloud scavenging of gases and particles, using scavenging coefficients.

[28] The EMEP Unified model use meteorological data from PARLAM [*Benedictow*, 2002], a dedicated version of the operational HIRLAM model (High Resolution Limited Area Model) maintained and verified at Norwegian Mete-

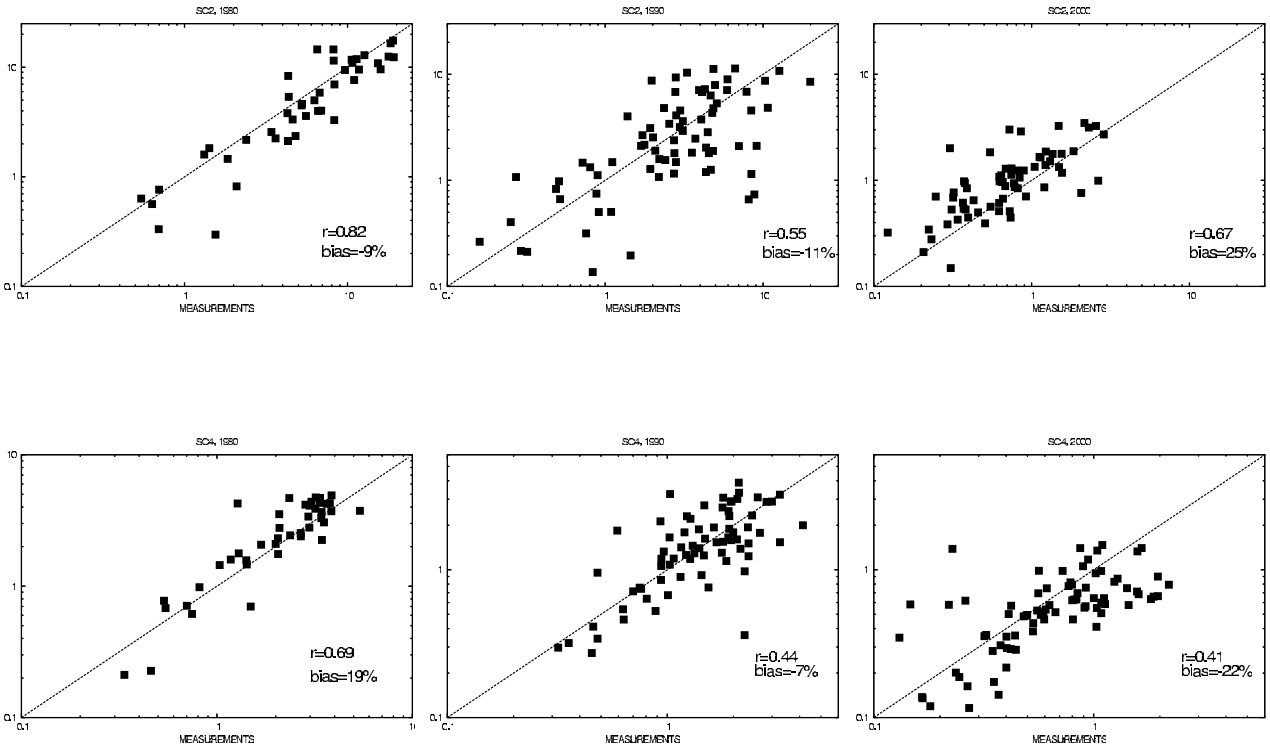


**Figure 2.** Scatterplots of EMEP model results versus measurements for (top) sulfur dioxide (ppbv) and (bottom) sulfate in air ($\mu$g(S)m$^3$) for 1980, 1990 and 2000.

orological Institute. The numerical solution of the advection term is based upon the fourth-order Bott scheme [*Bott*, 1989a, 1989b]. The lateral boundary conditions for most species are based on measurements as described by *Simpson et al.* [2003a] and *Fagerli et al.* [2004]. Furthermore, a scaling factor has been applied to account for the change in the concentrations at the boundary during the time period 1900–2000. This factor has been defined on the basis of the EPA emissions (*U.S. Environmental Protection Agency* [2000], and updates on their web page, http://www.epa.gov) for $SO_x$ and $NO_x$ emissions for the 1980–2000 period. The trends in ammonium aerosol were set by weighting the trend of $SO_x$ emissions with 2/3 and $NO_x$ emissions with 1/3, assuming that the production of ammonium nitrate and ammonium sulfate determines the trend. For the period prior to 1980, we have used the winter trends of sulfate and nitrate from an ice core at Col du Dome (4250 m asl, French Alps). In the winter time, Col du Dome is above the boundary layer most of the time. Most of the air pollution deposited at this site originates from sources outside the western boundary of the EMEP domain [*Fagerli et al.*, 2007], thus the trend extracted from the ice core is a good indicator of the air pollution arriving from North America. For ammonium, we used the trends of $NH_3$ emissions from United States derived from [*van Aardenne et al.*, 2001].

[29] For this study, the EMEP model is run for every tenth year for the period 1900–1980 plus 1985, 1990, 1995 and 2000 using appropriate boundary conditions and emissions. The meteorological year is 1997 for all the model runs. This was done because no set of meteorological data back to 1900 was available. Consequently, the interannual variability which has an important influence on sulfate aerosol distribution and its forcing could not be considered.

### 3.2. EMEP Model Evaluation

[30] Sulfur dioxide and sulfate background concentrations have been monitored in Europe at several sites since around 1980. Here, we briefly present model evaluation against $SO_2$ and $SO_4^{2-}$ measurements at the EMEP monitoring sites. For this evaluation we use the same model version revision 2.0, except that for the evaluated version the meteorology for the specific years has been applied (unlike in this study). Because of scarcity of continuous measurements from 1980 to 2000, and in order to evaluate the model's ability to reproduce the changes in sulfur levels over as large parts of Europe as possible, we use all the EMEP observations available in 1980, 1990 and 2000, respectively. Figure 2 shows scatterplots of model results versus observations for yearly averages of all the available EMEP sites measurements of sulfur dioxide and sulfate. The model tends to over predict the levels of sulfur dioxide somewhat in the recent years (bias = 25%), whilst in the beginning of the period the sulfur levels are underestimated by 9% on average. The opposite can be noted for sulfate, with model results 19% higher than the observations in 1980, and 22% lower in 2000. Sulfate in precipitation (not shown) behaves similar to sulfate in air. These results might indicate a too high $SO_2$ to $SO_4^{2-}$ oxidation rate in the beginning of the period and a too low oxidation rate in the end. However, there are other possible explanations. In general, the quality of both the emissions and the measurements have become better in recent years [e.g., *Vestreng et*

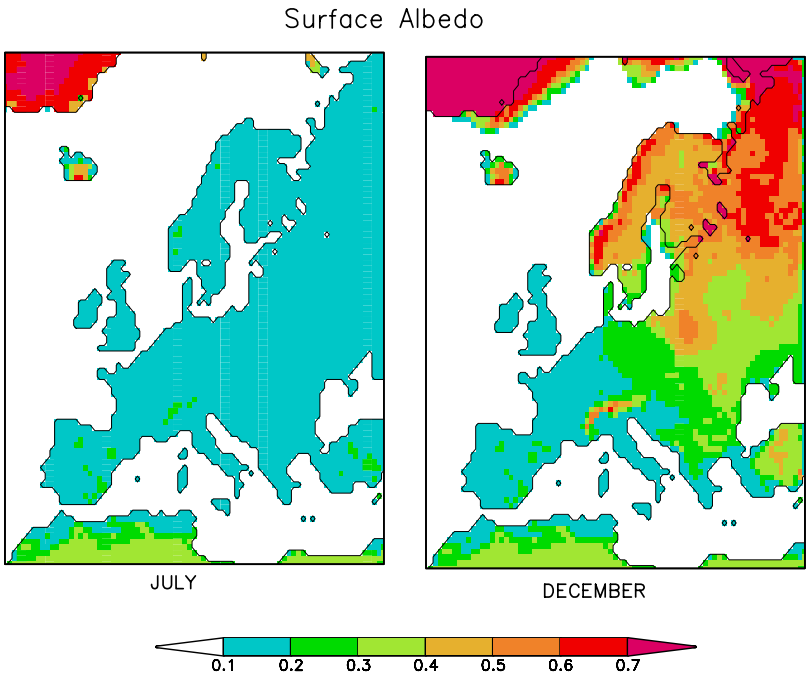


**Figure 3.** Mean modeled surface albedo for July and December 1997.

*al.*, 2007]. Moreover, the wet scavenging process is complicated and difficult to represent in atmospheric models, partly because of the uncertainty related to prediction of precipitation. In addition, the deposition of atmospheric $SO_2$ to plant surfaces stimulate the deposition of ammonia and vice versa, because of neutralizing effects [e.g., *van Hove et al.*, 1989; *Flechard et al.*, 1999]. The marked decrease in $SO_2$ emissions combined with small changes in $NH_3$ emissions implies a generally higher present-day dry deposition of $SO_2$ than at the time when $SO_2$ emissions peaked around 1980. This process has been parameterized and implemented in the EMEP model, but there is still too little experimental data to thoroughly validate the magnitude of this effect. In total, however, the EMEP model represents the downward trend in sulfur over Europe for the last decades fairly well. Evaluations of the EMEP model using all present-day EMEP measurement data are available elsewhere [e.g., *Fagerli et al.*, 2003; *Simpson et al.*, 2006; *Jonson et al.*, 2006; H. Fagerli et al., manuscript in preparation, 2007].

[31] In the work by *Fagerli et al.* [2007], modeled sulfate concentrations were compared to sulfate concentrations derived from long-term ice core records at Col du Dome (CDD, French Alps) and Colle Gnifetti (CG, Swiss Alps). The modeled sulfate trend and the inverted summer ice core record were found to be in excellent agreement for CDD with a weak increase between 1920 and 1950, a steep increase toward the maximum around 1980, and then a significant decrease over the last two decades. The source apportionment performed in the paper showed that the largest contributors to the depositions of sulfate both at CDD and CG were Spain, France, Germany and Italy. At CG, the simulations and ice record were found to be in reasonable agreement from 1920 to 1970. After 1970, the CG ice cores show a rather sudden decrease of concentrations, which was not found in the simulations, but this is possibly due to an artifact in the ice core record. In summary, the agreement between model simulations and the ice core records was rather encouraging and indicated that the historical emission inventories (at least for Spain, France, Germany and Italy) used for the study were reasonable.

### 3.3. Radiation Transfer Model

[32] The constructed trend of sulfate aerosol burden presented above was used as input for the Off-line Radiation Transfer Model (ORTM). A detailed model description is given by *Langmann et al.* [1998]. ORTM determines the direct and indirect shortwave forcing of sulfate aerosol based on the variable sulfate mass distribution and meteorological input data. The delta-Eddington approximation includes single as well as multiple scattering. Only the shortwave part of the solar spectrum, 0.2–5 $\mu$m, subdivided into 18 wavelength intervals, is considered, because sulfate aerosol has a negligible radiative effect in the infrared. Optical properties of dry sulfate aerosol are determined from Mie theory calculations, assuming a zero-order logarithmic size distribution n(r) [*Lenoble and Brogniez*, 1984], with a geometric mean particle radius $r_{gN}$ of 0.05 $\mu$m and a geometric standard deviation $\sigma_g$ of 1.8. The particle density was set to 1.6 $gcm^{-3}$, which is equivalent to a mean particle composition of 75% $H_2SO_4$ and 25% $H_2O$. The modification of aerosol specific extinction due to the relative humidity of the ambient air (RH) is considered using a simple approximation adapted from the data given by *Nemesure et al.* [1995]. For relative humidity (RH) below 80%, the specific extinction is enhanced by a factor of RH*0.04, assuming a minimum relative humidity of 25%. For relative humidity exceeding 80%, the specific extinction increases exponentially with RH. The factor 9.9 is reached

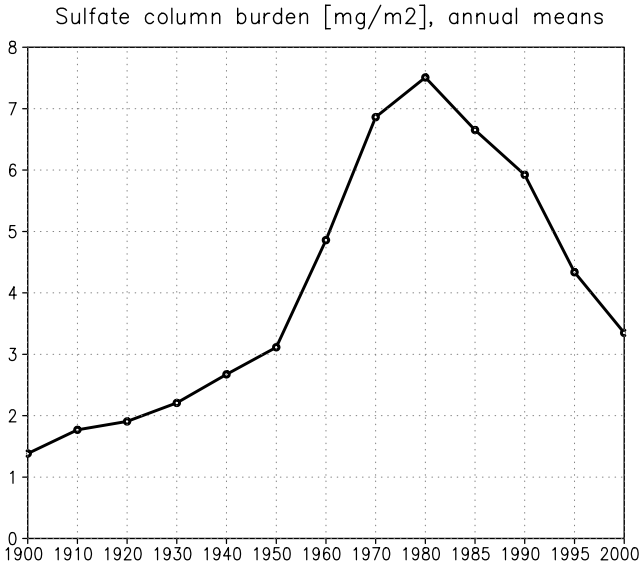


**Figure 4.** Total atmospheric sulfate load (mg($m^{-2}$)) over Europe, annual means, 1900–2000.

for RH = 100%. The single scattering albedo and the asymmetry factor are assumed to be independent of RH. This approach might result in a small overestimation of the shortwave radiative forcing of sulfate aerosol, because with increasing relative humidity forward scattering is increased and backscattering in space direction reduced (asymmetry factor increased).

[33] For this study, we have calculated the shortwave direct radiative forcing of the total sulfate aerosol (natural and anthropogenic), for all sky conditions at the top of the atmosphere (TOA). The meteorological parameters which have important impacts on the direct aerosol forcing, the cloud cover and the relative humidity, can be obtained from *Benedictow* [2005], the surface albedo is shown in Figure 3.

## 4. Historical Trends

### 4.1. European Atmospheric Load of Sulfate Aerosol

[34] The atmospheric load of sulfate over Europe increased from the 1900s to the 1980s because of expanding industrialization since the early 20th century and uncontrolled emissions of $SO_x$ (sulfur dioxide and sulfate). The sulfate load more than doubled during the first half of the century from 1.4 mg($m^{-2}$) sulfate in the 1900s to 3.1 mg($m^{-2}$) in the 1950s, with a very rapid growth in the following 20 years, when it again more than doubled reaching 6.7 mg($m^{-2}$) in the 1970s (Figure 4).

[35] The maximum annual mean of the total column burden was reached in the 1980s, with 7.5 mg($m^{-2}$) sulfate, more than 5 times higher than at the beginning of the century. The awareness of the health risks and environmental impacts of the atmospheric sulfate aerosol pollution resulted in emission control in western Europe in the 1980s, leading to a constant and significant reduction of anthropogenic $SO_x$ emissions [*Mylona*, 1996]. Eastern Europe followed suit in the 1990s. From the 1980s until the present, the sulfate load has been decreasing. The mean load in the year 2000 was 3.3 mg($m^{-2}$), slightly higher than in the 1950s.

[36] The modeled amount of oxidants, ozone ($O_3$), hydrogen peroxide ($H_2O_2$) and hydroxy radicals (OH), have changed considerably during the century. $O_3$ and $H_2O_2$ have increased by a factor of 2–3. OH has increased by a factor of 2.5 on average in the boundary layer (while it also decreased over some areas like UK, Belgium, and some marine areas affected by ship traffic). Few other studies on the historical trends in oxidants have been published [*Lelieveld et al.*, 2002; *Wang and Jacob*, 1998; *Berntsen et al.*, 1997]. The increase in OH since preindustrial times based on our model calculations is clearly larger than in, e.g., the work by *Wang and Jacob* [1998] who found an increase of 40–60% over land in the northern latitudes. Sensitivity runs show that the reason for the increase in OH is the increase in the $NO_x$/CO emission ratio from the 1900s. In this study, we have used $NO_x$ and CO emission inventories from different sources. In a test run, the $NO_x$ emissions for 1900 were scaled to the same level as the ones used by *van Aardenne et al.* [2001] (the same source as used for our CO emissions). In this run, modeled OH concentration for 1900 was considerably higher (resulting in an increase of OH from the 1900s to the 1980s of about 60% over continental Europe, but still with large regional differences). The effect on sulfate concentration for the 1900s is around 5–10%, but larger (15–20%) for the area around Sicily, where the oxidation of high volcanic emissions is limited by oxidants. In the beginning of the century, $SO_x$ emissions were low, and the level of oxidants was generally not a limitation for the oxidation to sulfate. The availability of oxidants becomes critical for the period when $SO_x$ emissions reached their maximum (1970s/1980s). Our CO and $NO_x$ emissions for this period stem from the same source (Table 2), hence the ratio is attributed to a lower uncertainty. We therefore conclude that the use of CO and $NO_x$ emissions from different sources is a minor source of uncertainty in our model study for sulfate.

### 4.2. European Direct Radiative Forcing

[37] The temporal pattern of the direct aerosol forcing directly reflects the pattern of sulfate aerosol burden. The forcing is negative, because sulfate aerosol particles scatter incoming shortwave radiation. The annual negative maximum of the forcing is seen in July, while the minimum is found in December (Figure 5). During winter months, solar radiation is very weak in high latitudes and the aerosol forcing is almost negligible. Like the atmospheric sulfate load, the direct radiative forcing increased from 1900 to 1980, it more than doubled between the 1950s and the 1970s. After 1980 the direct forcing steadily decreased. The monthly mean of the sulfate direct shortwave forcing over Europe was $-0.08$ W $m^{-2}$ in December 1900 and $-0.4$ W $m^{-2}$ in December 1980, from when it constantly decreased to $-0.2$ W $m^{-2}$ in December 2000, again comparable to December 1950. During summer, enhanced solar radiation results in a stronger forcing. The forcing is 5 to 7 times stronger in July than in December. The historical trend is much more pronounced in summer: from $-0.6$ W $m^{-2}$ in July 1900 the forcing increased to $-2.7$ W $m^{-2}$ in July 1980, and then it steadily decreased. In July 2000 the direct

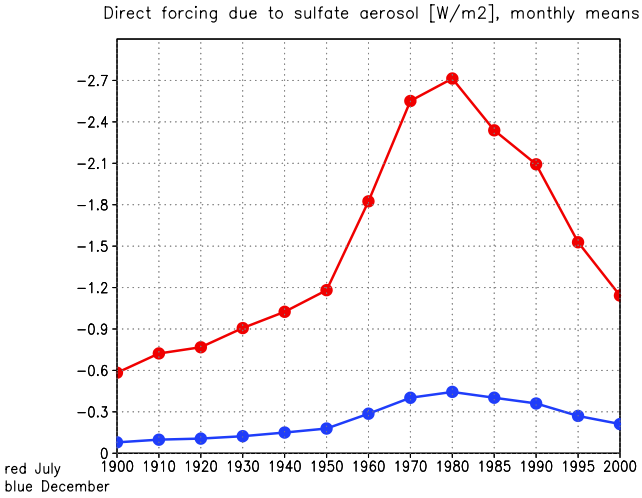


**Figure 5.** Direct shortwave radiative forcing due to sulfate aerosol (W $m^{-2}$) over Europe, 1900–2000, monthly means. Blue indicates December, and red indicates July.

sulfate forcing was reduced to −1.1 W $m^{-2}$, which is again comparable to the value in July 1950.

## 5. Regional Patterns of the Historical Trend

[38] In order to consider the regional aspects of the historical trend of the direct shortwave forcing of sulfate aerosol, we have analyzed the spatial evolution. The spatial evolution of the atmospheric load and the radiative forcing is discussed separately for winter (December, January, February) and for summer (June, July, August). Figure 6 illustrates the influence of the anthropogenic sulfate, showing the change in direct radiative forcing from 1900 to 1950 and from 1900 to 2000 for winter and summer, assuming that natural sources dominated the sulfate burden in 1900.

### 5.1. Winter

[39] During winter, photochemical processes responsible for the production of secondary pollutants are limited because of weak solar radiation intensity.

[40] In winter 1900, the highest atmospheric load can be found over central and southeastern Europe, mainly over Germany, with a seasonal mean over Germany of 5 mg($m^{-2}$)

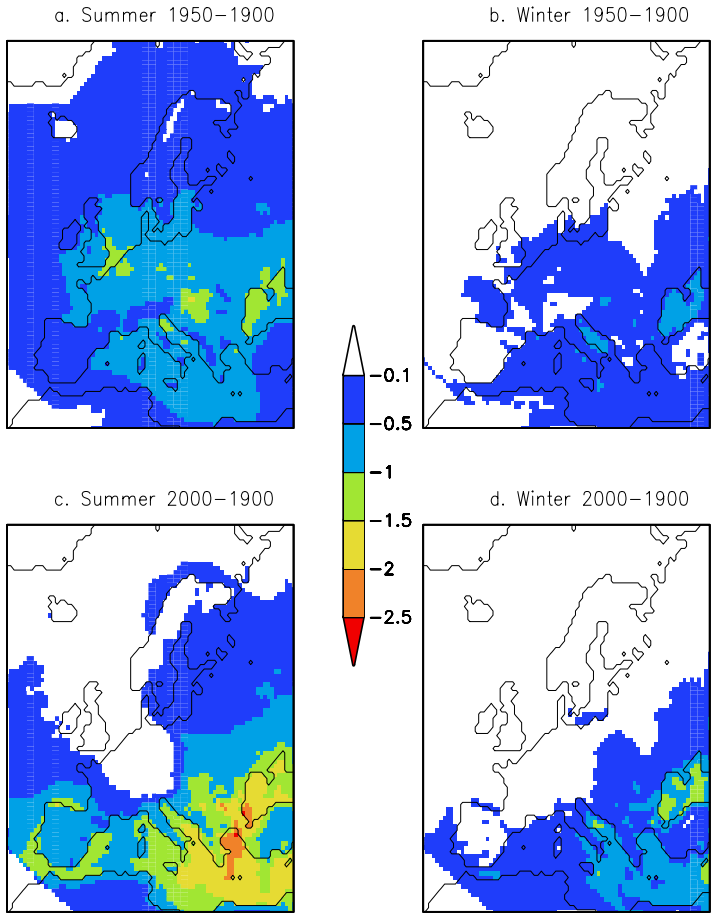


**Figure 6.** Change of the direct radiative sulfate aerosol forcing. (a) From 1900 to 1950, summer mean; (b) from 1900 to 1950, winter mean; (c) from 1900 to 2000, summer mean; and (d) from 1900 to 2000, winter mean.

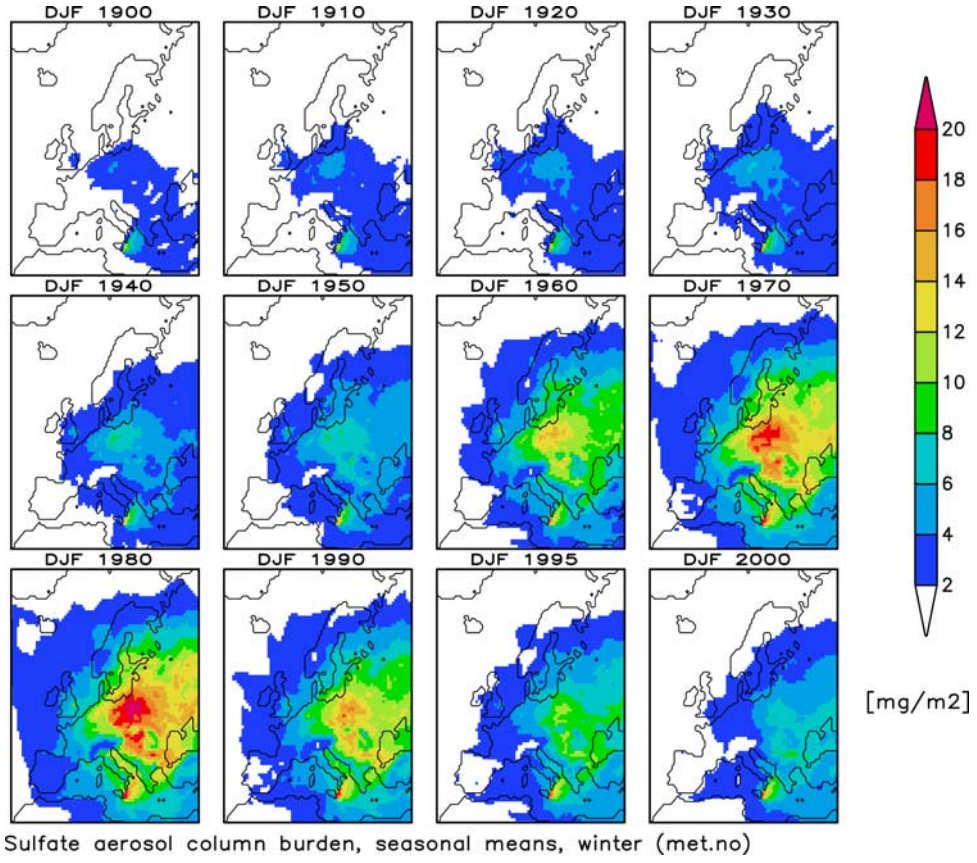


**Figure 7.** Wintertime horizontal distribution of the total atmospheric sulfate load (mg($m^{-2}$)), seasonal means, 1900–2000.

sulfate, compared with the mean European value of 1 mg($m^{-2}$) (Figure 7). A second maximum is located over the Mediterranean Sea, which originates from the volcanic degassing of Mount Etna, a point source producing about 13 mg($m^{-2}$) sulfate burden close to the source. The central European pollution maximum intensified and expanded northward, eastward and southward during the century. In the 1950s the maximum reached 7 mg($m^{-2}$), in the 1980s over 18 mg($m^{-2}$). The wintertime pollution over eastern Europe is mainly due to domestic heating with brown coal. The Mediterranean plume increased after the 1960s because of additional anthropogenic sources, including industry and traffic. During the 1980s, the European continent excluding northern Scandinavia and the Iberian Peninsula was very polluted during winter, with sulfate aerosol loads exceeding 14 mg($m^{-2}$) over most of the continent. The pollution maximum was shifted from Germany toward the east: Poland, western Soviet Union, Czechoslovakia, Yugoslavia, Hungary and Bulgaria. From the 1980s until the year 2000, the sulfate pollution was significantly reduced, with mean values of 3 mg($m^{-2}$) over western Europe, and 7 mg($m^{-2}$) over eastern and southern Europe and the eastern Mediterranean Sea. The mean European atmospheric load in winter 2000 is close to that of the 1950s, but the regional distribution is different. In winter of the 1950s the pollution maximum was located over Germany and Poland, whereas it was shifted south eastward toward the Black Sea during winter 2000.

[41] The spatial evolution of the wintertime direct sulfate forcing does not follow that of the atmospheric load (Figure 8). Because of weak radiation in the higher latitudes, the forcing is almost negligible in these regions. The forcing is concentrated in the lower latitudes, over areas with high atmospheric aerosol load, predominantly over the Black Sea and the Mediterranean Sea. The scattering effect of aerosols is increased over surfaces with low surface albedo such as water. From seasonal mean of $-0.3$ W $m^{-2}$ over these areas in 1900, it reached $-1.8$ W $m^{-2}$ over the Mediterranean Sea and $-2.5$ W $m^{-2}$ over the Black Sea in 1980. The mean December forcing in 2000 is slightly higher than in the 1950s, with a similar spatial pattern: It is concentrated in the lower latitudes with the strongest forcing observed over the Mediterranean Sea and the Black Sea. While some forcing is detectable over central Europe in winter in the 1950s, it is negligible in winter 2000. This is clearly due to reduced atmospheric load over western and central Europe in winter 2000 compared to the 1950s.

### 5.2. Summer

[42] During the summertime, photochemical processes responsible for the production of sulfate aerosol are enhanced because of strong solar radiation. In southern Europe, wet deposition is strongly limited by summertime aridity. These meteorological conditions cause pollution enhancement. Only in eastern Europe the summertime

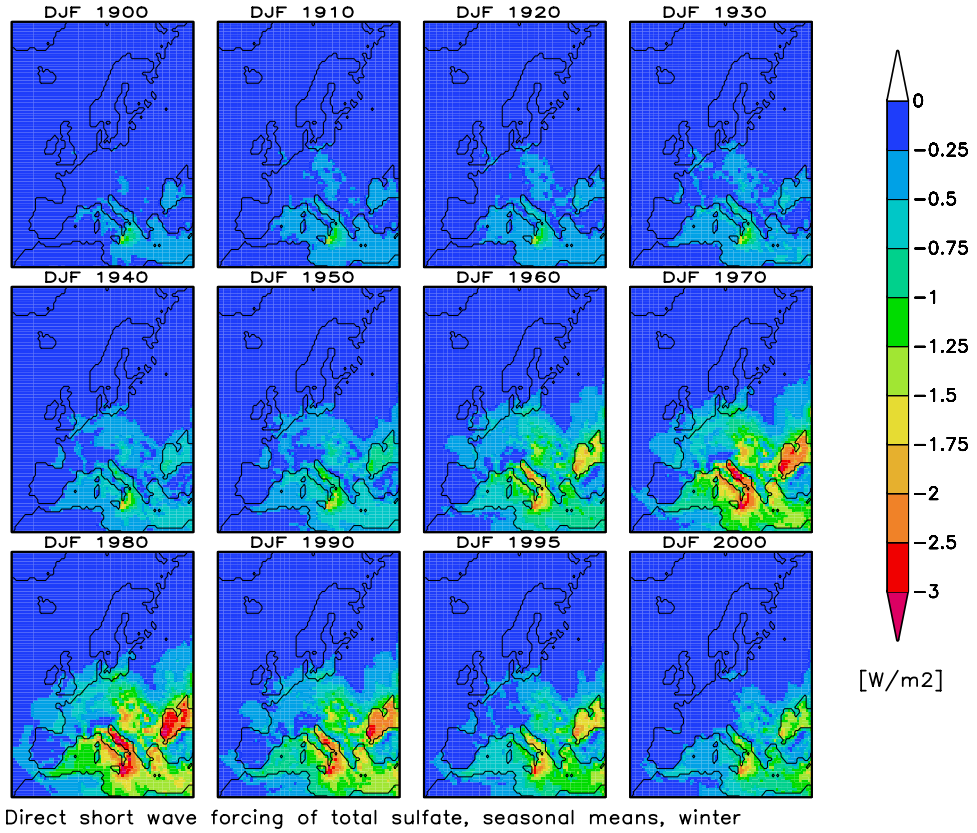


**Figure 8.** Wintertime direct radiative forcing due to sulfate aerosol (W $m^{-2}$), seasonal means, 1900–2000.

pollution is reduced, because there domestic heating is one of the main pollution sources.

[43] The spatial evolution of direct radiative forcing due to sulfate aerosol in summer is very similar to the spatial evolution of the sulfate atmospheric load (Figures 9 and 10). In summer 1900, two pollution maxima can be seen: one over northwestern Europe (Great Britain, Netherlands, Belgium, western Germany) and the North Sea and a second over the Mediterranean Sea. The northwestern plume intensified until the 1980s: The seasonal summertime mean increased from 6 mg($m^{-2}$) in 1900s to over 24 mg($m^{-2}$) in the 1980s; it expanded south eastward toward the Black Sea (Figure 9). The Black Sea was relatively unpolluted during summer in the first half of the century. The pollution enhanced rapidly from 3 mg($m^{-2}$) in the 1950s to 12 mg($m^{-2}$) in the 1980s. The Mediterranean pollution maximum expanded from the 1950s through the 1980s when the summertime mean value exceeded 22 mg($m^{-2}$). What we see now as a Sicilian plume is no longer dominated by the volcanic emissions from Mount Etna. The local anthropogenic emissions in Sicily peaked in the 1980s to become an important contributor to the plume. From the 1980s the summertime pollution over Europe began to decrease: The decrease of the Mediterranean plume is much slower than that of the plume over northwestern Europe. From 1995 on, the Mediterranean Sea is the most polluted area in summertime Europe. The main contributor to the summertime Mediterranean pollution nowadays are ship emissions. 54% of the total sulfate aerosol column burden over the Mediterranean in summer originates from ship emissions, contributing more than 50% of the direct radiative forcing [*Marmer and Langmann*, 2005].

[44] The spatial pattern of the aerosol burden in summer is very well reflected in the spatial evolution of the direct sulfate aerosol forcing (Figure 7). The forcing over the North Sea and western Europe enhanced steadily since the 1900s. Until the 1970s, the forcing was strongest over northwestern Europe with mean summer values exceeding $-6.5$ W $m^{-2}$. Afterward the forcing over the Mediterranean became dominant with values of up to $-6$ W $m^{-2}$. The forcing over the Black Sea was very high from 1970 until 1990. By the year 2000, the summer mean direct forcing over northwestern Europe was $-1.5$ to $-2$ W $m^{-2}$, while over the central Mediterranean Sea, particularly over the Aegean Sea, it reached $-3.5$ W $m^{-2}$. While the mean forcing in July 2000 has a similar value as July 1950, its maxima shifted from the North Sea to the Mediterranean Sea. In July 2000, the forcing over the North Sea was $-1.5$ W $m^{-2}$, compared to $-5$ W $m^{-2}$ in the 1950s.

### 5.3. Forcing Efficiency

[45] The concept of "forcing efficiency," defined as the ratio between the direct radiative forcing and the column burden was introduced by *Boucher and Anderson* [1995]. We found the modern European mean forcing efficiency to be $-230$ W(g sulfate)$^{-1}$. It is well within the range of mean global sulfate forcing efficiencies from different simulations and methods of $-130$ to $-370$ W(g sulfate)$^{-1}$ [*Seinfeld*, 2002]. In the AeroCom experiment, sulfate forcing efficien-

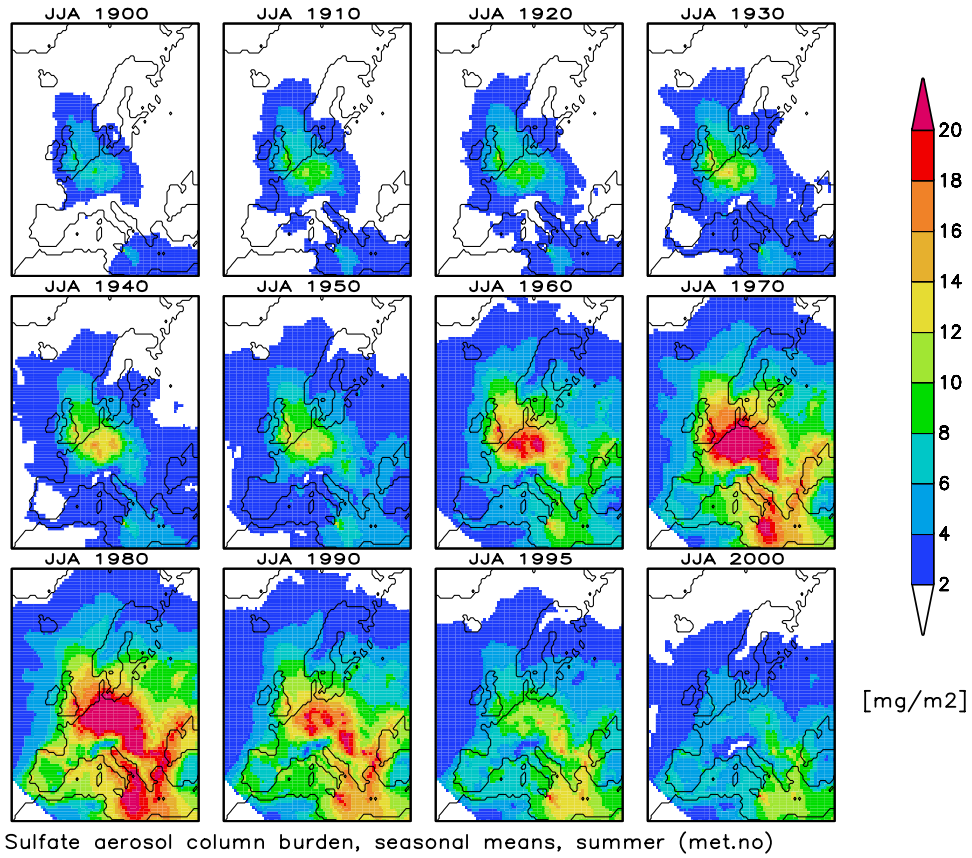


**Figure 9.** Summertime horizontal distribution of the total atmospheric sulfate load (mg($m^{-2}$)), seasonal means, 1900–2000.

cies have been predicted by different global models using prescribed $SO_x$ emissions, the global annual means ranging from −134 to −233 W(g sulfate)$^{-1}$ [*Schulz et al.*, 2006]. According to our findings, the forcing efficiency depends strongly on the season, the latitude and the surface albedo. In our model, the mean forcing efficiency is −78 W(g sulfate)$^{-1}$ in December and −335 W(g sulfate)$^{-1}$ in July, averaged from 1900–2000. These results qualitatively agree with the study of *Boucher and Anderson* [1995], with forcing efficiency of −62 W(g sulfate)$^{-1}$ for central Europe in January, and of −193 W(g sulfate)$^{-1}$ for July. *Boucher and Anderson* [1995] also found a pronounced negative correlation between the forcing efficiency and the cloud cover fraction. Climatological dependencies of the forcing efficiency could not be analyzed in this study, because the same meteorological year was used for all simulations. Additionally, the forcing efficiency depends the influence of the relative humidity on the aerosol optical properties. The forcing efficiency is not a temporally constant value. In December, the forcing efficiency in 2000 with −83 W(g sulfate)$^{-1}$ is higher than in the 1900s with −76 W(g sulfate)$^{-1}$ (Figure 11), because of the shift of sulfate aerosol burden maxima from higher to lower latitudes. The December forcing efficiency has a minimum of −69 W(g sulfate)$^{-1}$ in the 1960s. This is because the aerosol burden in the higher latitudes, which results in no or very low forcing during winter, initially increased faster than in the low latitudes. This trend was reversed since the 1960s. In July, the forcing efficiency is reduced from −363 in the 1900s to −305 W(g sulfate)$^{-1}$ in 2000. This reduction is caused by the shift of the pollution maxima from north to south. During the summertime, there are longer hours of daily solar radiation in the north, resulting in higher forcing efficiency. The annual mean forcing efficiency also slightly reduced from −246 to −230 W(g sulfate)$^{-1}$. The global mean historical forcing efficiency remained nearly constant in the work of *Boucher and Pham* [2002]. Probably, increased and decreased forcing tendencies compensate on the global mean.

### 5.4. Direct Forcing at Selected Areas

[46] Five different areas were selected to further illustrate different regional patterns of the direct radiative sulfate forcing: the English Channel, the Black Sea, Denmark, the Island of Sicily and Sonnblick, an Alpine mountain site.

[47] Surface albedo is lower over water than over land, resulting in stronger forcing efficiency over maritime areas. The present day forcing efficiency over the Black Sea is −385 W(g sulfate)$^{-1}$ in July and −190 W(g sulfate)$^{-1}$ in December, and over the English Channel −440 W(g sulfate)$^{-1}$ in July (Table 3).

[48] These values are much higher than the European mean. In winter, the English Channel receives less solar radiation than the Black Sea, resulting in lower efficiency of −70 W(g sulfate)$^{-1}$ in December. Seasonality is also very pronounced over Denmark, our most northern area, with strong forcing efficiency in July and weak in December.

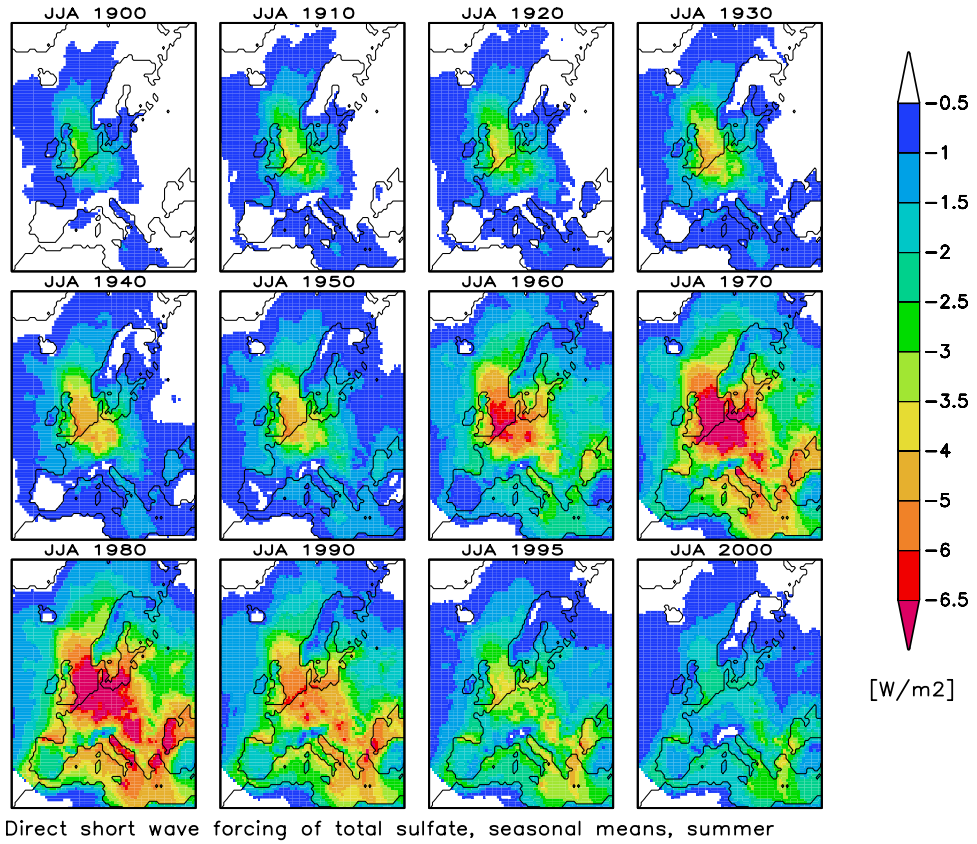


**Figure 10.** Summertime direct radiative forcing due to sulfate aerosol (W $m^{-2}$), seasonal means, 1900–2000.

[49] On the contrary, the forcing efficiency at the Island of Sicily, our most southern area, shows no pronounced seasonality (−190 W(g sulfate)$^{-1}$ in July and −157 W(g sulfate)$^{-1}$ in December). Relative to the European mean, the efficiency is low in summer, because of shorter days in the south than in the north, and high in winter, for the opposite reason. Over Sonnblick (3106 m asl) in December, the surface albedo of the snow covered mountains is high and the additional scattering by aerosols does not result in a significant forcing efficiency. The atmospheric burden of sulfate aerosol is the lowest at this elevated site; this site represents free tropospheric conditions. The resolution of the model results in a lower grid box elevation (2060 m asl), hence the simulated influence of the sulfate aerosol pollution from northwestern Europe is stronger than we would expect at this remote elevated region. The July forcing has a maximum in the 1985, and by the year 2000, this forcing is smaller than at the beginning of the century (Figure 12). The forcing over the English Channel, which is located close to strong sulfur emission sources, reaches −5.2 W $m^{-2}$ in the 1970s, by the year 2000 it also reduced close to the values of the 1900s. Similar trend can be found over Denmark. Comparing the trends over Sonnblick, Denmark and the English Channel to that over the Black Sea, reveals the shift of the forcing maxima from northwestern to southeastern Europe (section 5.3). The modern forcing over the Black Sea with −2.5 W $m^{-2}$ in July is 10 times stronger than at the beginning of the last century; the modern forcing in December is 5 times stronger than in the 1900s. The modern forcing over the Black Sea is similar to that in the 1960s, its reduction in the past 30 years less efficient than that of the European mean forcing. The forcing over Sicily shows the

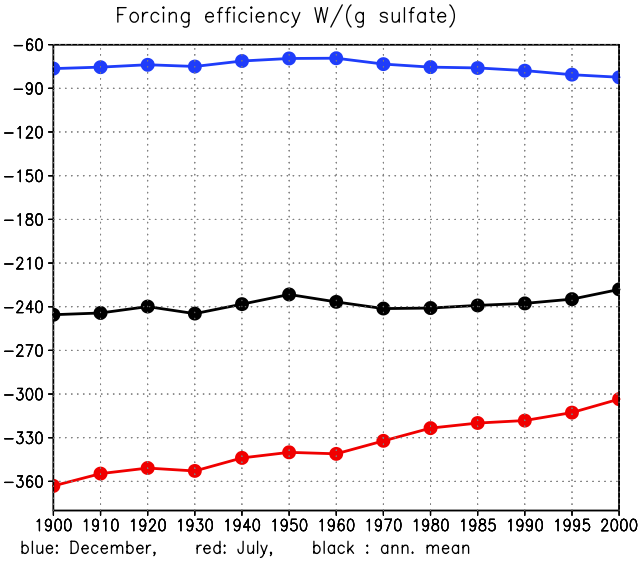


**Figure 11.** Historical trend in the forcing efficiency of sulfate aerosol over Europe (W(g sulfate)$^{-1}$), 1900–2000. Black indicates yearly mean, blue indicates monthly mean December, and red indicates monthly mean July.

**Table 3.** Forcing Efficiencies for the Selected Areas in July and in December 2000

| Area | Forcing Efficiency, W(g sulfate)$^{-1}$ | |
|---|---|---|
| | July 2000 | December 2000 |
| English Channel | −440 | −70 |
| Black Sea | −385 | −190 |
| Denmark | −360 | −72 |
| Sonnblick | −212 | −33 |
| Island of Sicily | −190 | −157 |
| European mean | −338 | −78 |

same trend as over the Black Sea, but the absolute values are much lower.

### 5.5. Contribution of Ship Emissions

[50] Unlike the land based sulfur emissions, which experienced significant reduction due to environmental policies since the 1980s, ship emissions keep increasing at an annual rate of ~2.5% (*Endresen et al.* [2003] and Table 1). The sensitivity study without ship emissions has showed, that their relative contribution to the direct radiative forcing over Europe has increased from 2% in the 1950s to 10% in 2000 (Figure 13). This contribution is especially relevant over the western Mediterranean [*Marmer and Langmann*, 2005] and southwest of the Gulf of Biskaya during summer, where it reaches 30% (Figure 14).

## 6. Summary and Conclusions

[51] We have provided an estimate of the historical evolution of the direct radiative forcing of sulfate aerosol over Europe, emphasizing on regional characteristics. The mean direct forcing has increased since the 1900s reaching its peak in the 1980s and then returning in present times to approximately the values of the 1950s. Despite the different distribution of the atmospheric load in December 1950 and 2000, the winter forcing distribution remains very similar, with maxima over the Black and the Mediterranean Seas. We found pronounced shift of the summer forcing maxima from northwestern to southeastern Europe. We can clearly observe that emission reductions, introduced in the 1980s, have led to a significant reduction in the atmospheric load and the direct forcing over Europe. The regional direct aerosol forcing depends not only on the sulfate load, but also on the latitude, the season, the cloud cover and the surface albedo. Ship emissions are found to increasingly contribute to sulfate aerosol burden and direct forcing, since their trend from the 1950s to 2000 is reverse to that of the land based emission sources.

[52] An uncertainty that needs to be carefully considered is the assumption of the same meteorological year [1997]

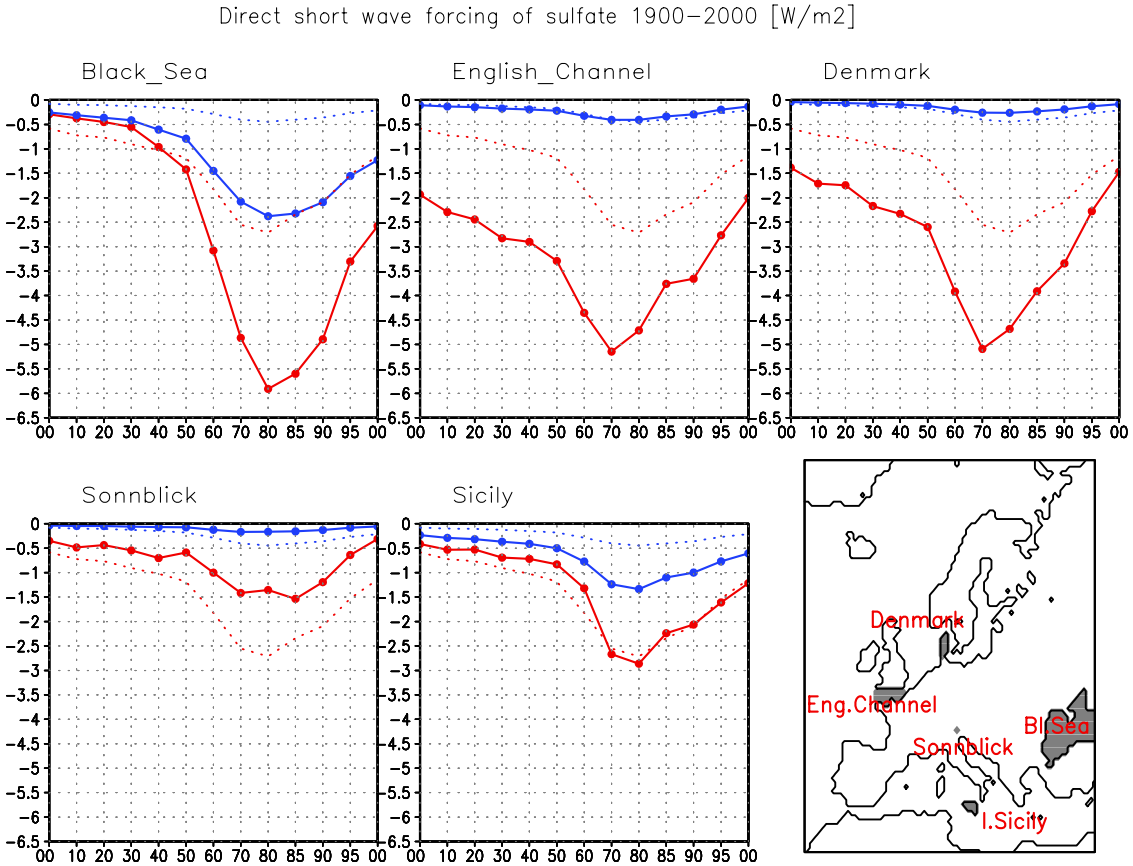


**Figure 12.** Historical trend of the direct sulfate forcing at the selected areas for July (red) and December (blue). Dotted lines show the trend of the European mean forcing in July (red) and December (blue). Also shown is a map of the selected areas.

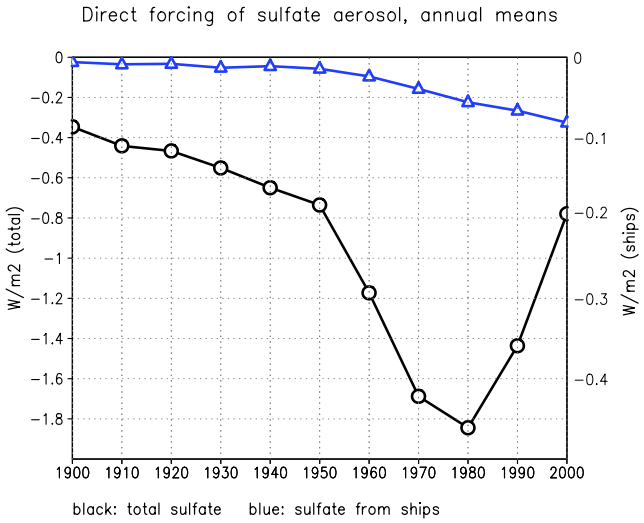


**Figure 13.** Historical trend of the direct radiative forcing due to total sulfate (black) and due to sulfate from ship emissions (blue).

for all simulations. Meteorological conditions play a very important role in aerosol production, transport and deposition [*Marmer and Langmann*, 2007] and can result in interannual concentration variabilities of up to 30% [*Putaud et al.*, 2004]. Furthermore, meteorology has an important impact on the forcing itself, via changes in surface albedo due to snow cover, changes in cloud cover and relative humidity of the ambient air. The aerosol forcing thus depends not only on the emissions strength, but also on interannual meteorological variability, which was not considered. For example, negative precipitation trends over areas with increasing emissions (central Europe and Mediterranean) as indicated in *IPCC* [2001b] might have resulted in higher atmospheric loads than modeled, while positive precipitation trends over Scandinavia and northern Russia could have the opposite effect. The trend in cloud cover [*Warren et al.*, 2007] follows that in precipitation, enhancing the forcing efficiency in areas with less clouds and vise versa. The forcing efficiency could have been further enhanced by the reduction of snow cover and glaciers over the past century [*Haeberli*, 2003; *Dyurgerov*, 1999]. All these trends are of regional character and their impacts interact with each other, we can only speculate on their impact on the historical sulfate aerosol forcing.

[53] Additional uncertainty is caused by the treatment of RH in the radiation model. In ORTM, size-dependent Mie calculations have been applied for dry aerosol particle size. The specific extinction obtained for a dry particle was then multiplied with a RH-dependent growth factor. This approach may underestimate the direct radiative forcing for high relative humidities.

[54] With black carbon to be included in future work, we expect different historical evolution of the aerosol forcing distribution and strength. Black carbon is highly absorbing and so its radiative forcing is positive in sign. Thus the forcings might partially offset each other. Historical changes of the aerosol single scattering albedo as an indicator of aerosol direct forcing due to changes in the aerosol composition for different regions are estimated by *Novakov et al.* [2003]. The nonlinearity of the aerosol burden response associated with emission changes as suggested by *Stier* [2005] can additionally affect the historical aerosol burden and the corresponding direct forcing when black carbon is included. On seasonal and regional scales the sign of the total forcing might vary substantially. Historical gridded emission inventory of carbonaceous aerosols for Europe needs to be established in order to complete the model simulations of the direct aerosol forcing evolution.

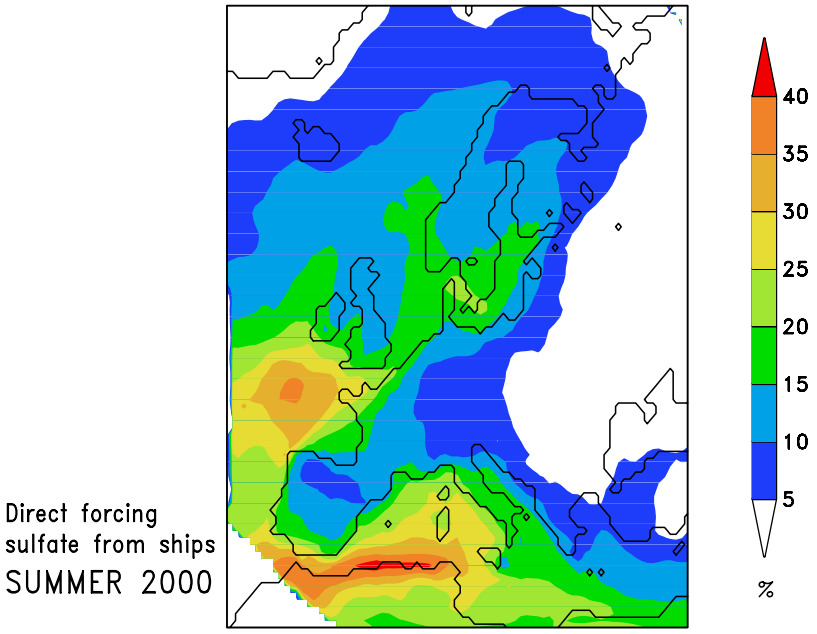


**Figure 14.** Seasonal mean of the relative contribution of sulfate from ships to the direct radiative forcing (%), summer 2000.

[55] **Acknowledgments.** We thank Stefan Kinne and Melissa Pfeffer for reviewing the manuscript internally. This research was financially supported by EU project CARBOSOL.

## References


Ackerman, A. S., B. O. Toon, D. E. Stevens, A. J. Heymfield, B. Ramanathan, and E. J. Welton (2000), Reduction of tropical cloudiness by soot, *Science*, *288*, 1042–1047.

Albrecht, B. (1989), Aerosols, cloud microphysics and fractional cloudiness, *Science*, *245*, 1227–1230.

Asman, W., and B. Drukker (1987), Modelled historical concentrations and depositions of ammonia and ammonium in Europe, *Atmos. Environ.*, *22*, 725–735.

Benedictow, A. (2002), 1999 meteorological fields produced by PARLAM-PS and used as input for Eulerian EMEP model. Documentation and characterization, technical report, Norw. Meteorol. Inst., Oslo.

Benedictow, A. (2005), Documentation and verification of the 1997 PARLAM-PS meteorological fields used as input for Eulerian EMEP model, technical report, pp. 63–64, 93–94, Norw. Meteorol. Inst., Oslo.

Berglen, T. F., G. Myhre, I. S. A. Isaksen, V. Vestreng, and S. Smith (2007), Sulphur trends in Europe: Are we able to model the recent observed decrease?, *Tellus*, in press.

Berntsen, T. K., I. S. A. Isaksen, G. Myhre, J. S. Fuglestvedt, F. Stordal, T. A. Larsen, R. S. Freckleton, and K. P. Shine (1997), Effects of anthropogenic emissions on tropospheric ozone and its radiative forcing, *J. Geophys. Res.*, *102*, 28,101–28,126.

Bott, A. (1989a), A positive definite advection scheme obtained by nonlinear re-normalization of the advection fluxes, *Mon. Weather Rev.*, *117*, 1006–1016.

Bott, A. (1989b), Reply in "Notes and Correspondence," *Mon. Weather Rev.*, *117*, 2633–2636.

Boucher, O., and T. L. Anderson (1995), General circulation model assessment of the sensitivity of direct climate forcing by anthropogenic sulfate aerosols to aerosol size chemistry, *J. Geophys. Res.*, *100*, 26,117–26,134.

Boucher, O., and M. Pham (2002), History of sulfate aerosol radiative forcings, *Geophys. Res. Lett.*, *29*(9), 1308, doi:10.1029/2001GL014048.

Brimblecombe, P. (1987), *The Big Smoke: A History of Air Pollution in London Since Medieval Times*, Methuen, New York.

DeMott, P. J., Y. Chen, S. M. Kreidenweis, D. C. Rogers, and D. E. Sherman (1999), Ice formation by black carbon particles, *Geophys. Res. Lett.*, *26*(16), 2429–2432.

Dyurgerov, M. (1999), Mountain and subpolar glaciers show an increase in sensitivity to climate warming and intensification of the water cycle, *J. Hydrol.*, *282*, 2429–2432.

Endresen, O., E. Sørgård, J. Sundet, S. Dalsøren, I. Isaksen, T. Berglen, and G. Gravir (2003), Emission from international sea transportation and environmental impact, *J. Geophys. Res.*, *108*(D17), 4560, doi:10.1029/2002JD002898.

Fagerli, H., D. Simpson, and W. Aas (2003), Model performance for sulphur and nitrogen compounds for the period 1980 to 2000, in *Transboundary Acidification, Eutrophication and Ground Level Ozone in Europe*, *EMEP Status Rep. 1/2003*, part II, *Unified EMEP Model Performance*, edited by L. Tarrasón, pp. 1–66, Norw. Meteorol. Inst., Oslo.

Fagerli, H., D. Simpson, and S. Tsyro (2004), Unified EMEP model: Updates, in *Transboundary Acidification, Eutrophication and Ground Level Ozone in Europe*, *EMEP Rep. 1/2004*, pp. 11–18, Norw. Meteorol. Inst., Oslo.

Fagerli, H., M. Legrand, S. Pruenkert, D. Simpson, V. Vestreng, and M. Cerqueira (2007), Modeling historical long-term trends of sulfate, ammonium, and elemental carbon over Europe: A comparison with ice core records in the Alps, *J. Geophys. Res.*, doi:10.1029/2006JD008044, in press.

Flechard, C. R., D. Fowler, M. A. Sutton, and J. N. Cape (1999), A dynamic chemical model of bi-directional ammonia exchange between semi-natural vegetation and the atmosphere, *Q. J. R. Meteorol. Soc.*, *125*, 2611–2641.

Friedrich, F., and E. Reis (Eds.) (2004), *Emissions of Air Pollutants-Measurements, Calculations and Uncertainties*, Springer, New York.

Haeberli, W. (2003), Spuren des Hityesommers 2003 im Eis der Alpen, submission to the Parliament of Switzerland, Bern.

Haywood, J. M., D. L. Robert, A. Slingo, J. M. Edwards, and K. P. Shine (1997), General circulation model calculations of the direct radiative forcing by anthropogenic sulfate and fossil-fuel soot aerosol, *J. Clim.*, *10*, 1562–1577.

Intergovernmental Panel on Climate Change (2001a), *Climate Change 2001: The Scientific Basis*, Cambridge Univ. Press, New York.

Intergovernmental Panel on Climate Change (2001b), *Climate Change 2001: Impacts, Adaptation and Vulnerability*, Cambridge Univ. Press, New York.

Jonson, J., D. Simpson, H. Fagerli, and S. Solberg (2006), Can we explain the trends in European ozone levels?, *Atmos. Chem. Phys.*, *6*, 51–66.

Krüger, O., and H. Grassl (2002), The indirect aerosol effect over Europe, *Geophys. Res. Lett.*, *29*(19), 1925, doi:10.1029/2001GL014081.

Langmann, B., M. Herzog, and H. F. Graf (1998), Radiative forcing of climate by sulfate aerosols as determined by a regional circulation chemistry transport model, *Atmos. Environ.*, *32*, 2757–2768.

Lefohn, S., J. Husar, and R. Husar (1999), Estimating historical anthropogenic global sulphur emission patterns for the period 1850–1990, *Atmos. Environ.*, *33*, 3435–3444.

Lelieveld, J., W. Peters, F. J. Dentener, and M. C. Krol (2002), Stability of tropospheric hydroxyl chemistry, *J. Geophys. Res.*, *107*(D23), 4715, doi:10.1029/2002JD002272.

Lenoble, J., and C. Brogniez (1984), A comparative review of radiation aerosol models, *Contrib. Atmos. Phys.*, *57*, 1–20.

Lesins, G., P. Chylek, and U. Lohmann (2002), A study of internal and external mixing scenarios and its effect on aerosol optical properties and direct radiative forcing, *J. Geophys. Res.*, *107*(D10), 4094, doi:10.1029/2001JD000973.

Lloyd's Register of Shipping (1995), Marine exhaust emissions research programme, London.

Lloyd's Register of Shipping (1998), Marine exhaust emissions quantification study-Baltic Sea, *Final Rep. 98/EE77036*, London.

Lloyd's Register of Shipping (1999), Marine exhaust emissions quantification study for the Mediterranean Sea, *Rep. 99/EE/7044*, London.

Marmer, E., and B. Langmann (2005), Impact of ship emissions on Mediterranean summertime pollution and climate: A regional model study, *Atmos. Environ.*, *39*, 4659–4669.

Marmer, E., and B. Langmann (2007), Aerosol modeling over Europe: 1. Interannual variability of aerosol distribution, *J. Geophys. Res.*, doi:10.1029/2006JD008113, in press.

Metzger, S., F. Dentener, S. Pandis, and J. Lelieveld (2002a), Gas/aerosol partitioning: 1. A computationally efficient model, *J. Geophys. Res.*, *107*(D16), 4312, doi:10.1029/2001JD001102.

Metzger, S., F. Dentener, M. Krol, A. Jeuken, and J. Lelieveld (2002b), Gas/aerosol partitioning: 2. Global modeling results, *J. Geophys. Res.*, *107*(D16), 4313, doi:10.1029/2001JD001103.

Mitchell, B. (1981), *European Historical Statistics 1750–1975*, 2nd revised ed., Macmillan Press Ltd., New York.

Myhre, G., F. Stordal, K. Restad, and I. S. Isaksen (1998), Estimates of the direct radiative forcing due to sulfate and soot aerosols, *Tellus, Ser. B*, *50*, 463–477.

Myhre, G., A. Myhre, and F. Stordal (2001), Historical evolution of radiative forcing of climate, *Atmos. Environ.*, *35*, 2361–2373.

Mylona, S. (1996), Sulphur dioxide emissions in Europe 1880–1991 and their effect on sulphur concentrations and depositions, *Tellus, Ser. B*, *48*, 662–689.

Nemesure, S., R. Wagner, and S. E. Schwartz (1995), Direct shortwave forcing of climate by the anthropogenic sulfate aerosol: Sensitivity to particle size, composition and relative humidity, *J. Geophys. Res.*, *100*, 26,105–26,116.

Novakov, T., V. Ramanathan, J. E. Hansen, T. W. Kirchstetter, M. Sato, J. E. Sinton, and J. A. Sathaye (2003), Large historical changes of fossil-fuel black carbon aerosols, *Geophys. Res. Lett.*, *30*(6), 1324, doi:10.1029/2002GL016345.

Putaud, J., et al. (2004), A European aerosol phenomenology-2: chemical characteristics of particulate matter at kerbside, urban, rural and background sites in Europe, *Atmos. Environ.*, *38*, 2579–2595.

Schulz, M., et al. (2006), Radiative forcing by aerosols as derived from the AeroCom present-day and pre-industrial simulations, *Atmos. Chem. Phys.*, *6*, 5225–5246.

Seinfeld, J. H. (Ed.) (2002), Direct aerosol forcing, paper presented at Air Pollution as a Climate Forcing: A Workshop, Goddard Inst. for Space Stud., New York.

Simpson, D., H. Fagerli, J. Jonson, S. Tsyro, P. Wind, and J.-P. Tuovinen (2003a), The EMEP Unified Eulerian Model. Model description, *EMEP MSC-W Rep. 1/2003*, Norw. Meteorol. Inst., Oslo.

Simpson, D., J.-P. Tuovinen, L. Emberson, and M. Ashmore (2003b), Characteristics of an ozone deposition module II: Sensitivity analysis, *Water Air Soil Pollut.*, *143*, 123–137.

Simpson, D., H. Fagerli, S. Hellsten, K. Knulst, and O. Westling (2006), Comparison of modelled and monitored deposition fluxes of sulphur and nitrogen to ICP-forest sites in Europe, *Biogeosciences*, *3*(3), 337–355.

Smith, E., D. Andres, E. Conception, and J. Lurz (2004), Historical sulfur dioxide emissions 1850–2000: Methods and results, *PNNL Res. Rep. 14537*, Pacific Northwest Natl. Lab., Richland, Wash.

Stier, P. (2005), Towards the assessment of the aerosol radiative effects: A global modelling approach, Ph.D. thesis, Max-Planck-Inst. for Meteorol., Hamburg, Germany.

Tarrasón, L., S. Turner, and I. Floisand (1995), Estimation of seasonal dimethyl sulphide fluxes over the North Atlantic Ocean and their contribution to European pollution levels, *J. Geophys. Res.*, *100*, 11,623–11,639.

Tegen, I., D. Koch, A. L. Lacis, and M. Sato (2000), Trends in tropospheric aerosol loads and corresponding impact on direct radiative forcing between 1950 and 1990: A model study, *J. Geophys. Res.*, *105*, 26,971–26,989.

Tuovinen, J.-P., M. Ashmore, L. Emberson, and D. Simpson (2004), Testing and improving the EMEP ozone deposition module, *Atmos. Environ.*, *38*, 2373–2385.

Twomey, S. (1974), Pollution and the planetary albedo, *Atmos. Environ.*, *8*, 1251–1256.

U.S. Environmental Protection Agency (2000), National air pollutant emission trends: 1900–1998, *EPA 454/R-00-002*, Washington, D. C.

van Aardenne, J., F. Dentener, J. Olivier, C. Goldewijk, and J. Lelieveld (2001), A 1 × 1 degree resolution data set of historical anthropogenic trace gas emissions for the period 1890–1990, *Global Biogeochem. Cycles*, *15*, 909–928.

van Hove, L. W. A., E. H. Adema, W. J. Vredenberg, and G. A. Pieters (1989), A study of the adsorption of $NH_3$ and $SO_2$ on leaf surfaces, *Atmos. Environ.*, *23*(7), 1479–1486.

Vestreng, V., M. Adams, and J. Goodwin (2004), Inventory review 2004. Emission data reported to CLRTAP and under the NEC directive, EMEP/EEA Joint Review Report, *Tech. Rep. EMEP-MSCW Rep. 1/2004*, Norw. Meteorol. Inst., Oslo.

Vestreng, V., G. Myhre, H. Fagerli, S. Reis, and L. Tarrasn (2007), Twenty-five years of continuous sulphur dioxide emission reduction in Europe, *Atmos. Chem. Phys.*, *7*, 3663–3681.

Wang, Y., and D. J. Jacob (1998), Anthropogenic forcing on tropospheric ozone and OH since preindustrial times, *J. Geophys. Res.*, *103*(D23), 31,123–31,135.

Warren, S. G., R. M. Eastman, and C. J. Hahn (2007), A survey of changes in cloud cover and cloud types over land from surface observations, 1971–1996, *J. Clim.*, *20*(4), 717–738.

Whall, C., D. Cooper, K. Archer, L. Twigger, N. Thurston, D. Ockwell, A. McIntyre, and A. Ritchie (2002), Quantification of emissions from ships associated with ship movements between ports in the European Community, European commission final report, Entec UK Limited, Northwich, U. K.

H. Fagerli and V. Vestreng, Norwegian Meteorological Institute, N-0313 Oslo, Norway. (hilde.fagerli@met.no; vigdis.vestreng@met.no)

B. Langmann, Department of Experimental Physics, National University of Ireland, Galway, Ireland. (baerbel.langmann@zmaw.de)

E. Marmer, Institute for Environment and Sustainability, European Commission-Joint Research Centre, I-21020 Ispra, Italy. (elina.marmer@jrc.it)